Evaluation of Techniques to Estimate Titan III-C Flight Loads

MICHAEL H. MARX*
Lincoln Laboratory, Lexington, Mass.
AND
ARCHIBALD W. ADKINS†
Littleton Research and Engineering Corporation, Littleton, Mass.
AND
LOUIS L. BUCCIARELLI‡ AND DAVID C. HYLAND§
Massachusetts Institute of Technology, Cambridge, Mass.

Two techniques to predict satellite boost phase inertia loads are evaluated. The first is a straightforward application of Fourier transforms. The input data are known spectra of the booster/payload interface accelerations and forecast payload transfer functions, based on anticipated payload dimensions, mass distribution, and important modes, frequencies and damping. Application to a multidegree-of-freedom system is demonstrated. The second approach models the interface accelerations as a superpositioning of a finite number of enveloped narrowband excitations whose center frequencies lie at the lower natural frequencies of the booster. The envelope functions reflect the transient, nonstationary character of the excitation. Assuming the envelope to be "slowly varying," obtaining the mean square modal response of the satellite is relatively simple.

Nomenclature

x,y,z	= Cartesian coordinate axes attached to the booster/payload interface
$\theta_x,\theta_y,\theta_z$	= rotations about the x, y, z axes
$\bar{u}_j,\bar{v}_j,\bar{w}_j$	= components of jth particle transport displacement
u_j,v_j,w_j	= components of jth particle relative displacement
$[\ m\ ]$	= mass particle matrix (diagonal matrix)
$[\phi]$	= modal matrix
$[G]$	= matrix representing the payload geometry
$[\Gamma]$	= weighting matrix
$\{s\}$	= particle transport displacement vector
$\{S\}$	= interface transport displacement vector
$\{r\}$	= particle relative displacement vector
$\{\delta\}$	= modal transport displacement vector
$\{\xi\}$	= modal relative displacement vector
M_k	= generalized mass of kth mode
$U,V,W,\Theta_x,\Theta_y,\Theta_z$	= Fourier transforms of $\bar{u}_0(t)$, $\bar{v}_0(t)$, $\bar{w}_0(t)$, $\theta_x(t)$, $\theta_y(t)$, $\theta_z(t)$
Ξ_k	= Fourier transform of $\xi_k(t)$
H_k	= system transfer function for relative motion for the kth mode
I_k	= Fourier transform of the kth mode input displacements
$f(t)$	= a time dependent forcing function
$g(t)$	= a deterministic, slowly varying envelope function
$n(t)$	= a stationary, narrowband random process
$h(t, t_i)$	= impulse response
$E[\ \ ]$	= expected value
N	= total number of modes retained
R_0, μ	= parameters describing the nature of the narrowband, stationary process
Ω	= center frequency of the enveloped, narrowband excitation
ω	= circular frequency, rad/sec
ω_k	= natural frequency of the kth mode
ω_d	= damped natural frequency
λ	= Ω/ω_k
ζ	= damping ratio
ε	= a constant $\ll 1$. taken $= \zeta$
β	= $(\lambda - 1)/\zeta$
τ, η	= slow time variables

Presented as Paper 70-485 at the AIAA 3rd Communications Satellite Systems Conference, Los Angeles, Calif., April 6–8, 1970; submitted February 1, 1971; revision received October 12, 1971. This work was sponsored by the Department of the Air Force.

Index categories: Structural Dynamic Analysis; Spacecraft Configurational and Structural Design (Including Loads); Spacecraft and Component Ground Testing and Simultation.

* Staff Member.
† Chief Staff Engineer.
‡ Associate Professor of Aeronautics and Astronautics.
§ Research Assistant. Member AIAA.

Introduction

THE structural design of a satellite in the Lincoln Experimental Satellite (LES) program was originally based on its random vibration specification. The specified input acceleration power spectral density was an envelope of observed spectra and, hence, represented an rms acceleration much greater than that for any individual flight. Notching at satellite natural frequencies was not permitted, and the resulting 3σ values for response accelerations at some points of the satellite were of the order of $100g$. These results led to excessively conservative design as demonstrated by more recent analysis[1] which indicated the satellites should have been designed for accelerations of the order of $10g$.

The random vibration specification was abandoned for LES-5, launched July 6, 1967. Structural qualification was based on a dynamic analysis of the dispenser truss plus all satellites. The natural modes and frequencies and mass distribution of each satellite were given to Martin Marietta Corporation engineers who then determined the dynamic characteristics of the payload and found the system response to excitations from records of 27 engine firings. In other words, they solved the differential equations of motion for 27 forcing functions each consisting of the six acceleration components of the booster/payload interface taken as a plane rigid body. These accelerations were concluded to be virtually independent of payload impedance for payloads in a given weight category.[2]

Although this procedure is satisfactory to verify structural adequacy of the payload, its results become available too late to be useful in satellite design. The structural design of the satellite must often be completed long before the nature of the rest of the payload is known. The difficulty of estimating design loads under such circumstances led to the two studies reported here.

One of these studies is a straightforward analysis, in the frequency domain, of the response of a given system to excitations obtained from Titan III-C test records and analyses. This study shows the advantages of this approach (over analysis in the time domain) for estimating flight loads at the design stage.

The other study models the interface accelerations as a superpositioning of a finite number of enveloped, narrowband excitations whose center frequencies lie at the lower natural frequencies of the booster. The envelope functions reflect the transient, nonstationary character of the excitation. Assuming the envelope to be "slowly varying," obtaining the mean square modal response of the satellite is relatively simple.

Analysis in the Frequency Domain

Formulation

In this formulation the payload is modeled as a lumped parameter system. Motion of the support, which represents the booster/payload interface, provides the input excitation to the system. The absolute displacement of the lumped masses is $\{s\}+\{r\}$.

Transformation to modal coordinates is accomplished via

$$\{r\}=[\phi]\{\xi\} \qquad (1)$$

$$\{s\}=[\phi]\{\delta\} \qquad (2)$$

For the usual case where the damping matrix is some linear combination of the mass and stiffness matrices, this transformation uncouples the equations of motion. The transformed equations are

$$\ddot{\xi}_k+2\zeta_k\omega_k\dot{\xi}_k+\omega_k{}^2\xi_k=-\ddot{\delta}_k \qquad k=1,2\ldots N \qquad (3)$$

where

$$\delta_k=(1/M_k)\{\phi_k\}^T[\ m\ ]\{s\} \qquad (4)$$

The particle transport displacement vector can be written

$$\{s\}=\begin{Bmatrix}\bar{u}_1\\ \bar{v}_1\\ \bar{w}_1\\ \bar{u}_2\\ \bar{v}_2\\ \bar{w}_2\\ \cdot\\ \cdot\\ \cdot\end{Bmatrix}=\begin{bmatrix}1&0&0&0&z_1&-y_1\\ 0&1&0&-z_1&0&x_1\\ 0&0&1&y_1&-x_1&0\\ 1&0&0&0&z_2&-y_2\\ 0&1&0&-z_2&0&x_2\\ 0&0&1&y_2&-x_2&0\\ \cdot&\cdot&\cdot&\cdot&\cdot&\cdot\\ \cdot&\cdot&\cdot&\cdot&\cdot&\cdot\\ \cdot&\cdot&\cdot&\cdot&\cdot&\cdot\end{bmatrix}\begin{Bmatrix}\bar{u}_0\\ \bar{v}_0\\ \bar{w}_0\\ \theta_x\\ \theta_y\\ \theta_z\end{Bmatrix}$$

$$=[G]\{S\} \qquad (5)$$

where $[G]$ is a matrix representing the payload geometry and $\{S\}$ contains the components of the rigid body displacement of the booster/payload interface.

Using Eq. (5), Eq. (4) becomes

$$\delta_k=(1/M_k)\{\phi_k\}^T[\ m\ ][G]\{S\}=\{\Gamma_k\}^T\{S\} \qquad (6)$$

and Eq. (3) takes the form

$$\ddot{\xi}_k+2\zeta_k\omega_k\dot{\xi}_k+\omega_k{}^2\xi_k=-\Gamma_{\bar{u}k}\ddot{\bar{u}}_0-\Gamma_{\bar{v}k}\ddot{\bar{v}}_0-\cdots-\Gamma_{\theta_{zk}}\ddot{\theta}_z \qquad (7)$$

The customary formulas[3] exhibiting the reversibility of the Fourier transform are

$$F(\omega)=\int_{-\infty}^{\infty}f(t)e^{-i\omega t}dt \qquad (8)$$

$$f(t)=\frac{1}{2\pi}\int_{-\infty}^{\infty}F(\omega)e^{i\omega t}d\omega \qquad (9)$$

Multiplying Eq. (7) by $e^{-i\omega t}$, integrating, and solving for $\Xi_k(\omega)$ yields

$$\Xi_k(\omega)=H_k(\omega)I_k(\omega) \qquad (10)$$

where

$$H_k(\omega)=\frac{(\omega/\omega_k)^2}{1-(\omega/\omega_k)^2+i2\zeta_k(\omega/\omega_k)} \qquad (11)$$

and

$$I_k(\omega)=\Gamma_{\bar{u}k}U_0(\omega)+\Gamma_{\bar{v}k}V_0(\omega_k)+\cdots+\Gamma_{\theta_{zk}}\Theta z(\omega) \qquad (12)$$

$H_k(\omega)$ is the familiar transfer function for relative motion and $I_k(\omega)$ the Fourier transform of the kth mode input displacements.

By way of Eq. (9)

$$\xi_k(t)=\frac{1}{2\pi}\int_{-\infty}^{\infty}H_k(\omega)I_k(\omega)e^{i\omega t}d\omega \qquad (13)$$

Differentiation of a time function corresponds to multiplication of its transform by $i\omega$. Therefore,

$$\ddot{\xi}_k(t)=\frac{1}{2\pi}\int_{-\infty}^{\infty}H_k(\omega)[-\omega^2I_k(\omega)]e^{i\omega t}d\omega \qquad (14)$$

The transfer function is unchanged whether input and response functions are both displacements or both accelerations.

Ordinarily the input data are acceleration time histories rather than displacement time histories. Under these circumstances, it is easiest to compute the transforms of the accelerations directly. This, in essence, multiplies each term of Eq. (12) by $-\omega^2$ and leads straight to Eq. (14). However, it is a simple matter to find either the displacement or the acceleration response time history [Eq. (13) or Eq. (14)] or both.

Example A

Three 500-lb mass particles mounted on a uniform beam at 50-in. intervals demonstrate the application of this theory. Although this model is too simple to represent an actual Titan III-C payload, it nevertheless serves for a useful preliminary study of the response of payload lateral bending modes.

The response of a payload to a given excitation is determined completely by the mass distribution, natural modes and frequencies, and damping ratios (Table 1). The mode shapes were calculated, together with the natural frequencies, for an arbitrary constant value of beam stiffness (EI). The frequencies were then multiplied by a constant to make 15.0 Hz the first natural frequency for case 1 and by another constant to make 20.3 Hz the first natural frequency for case 2. It is anticipated that these natural mode shapes will be assigned arbitrarily in later studies (subject to the orthogonality conditions).

In this example, excitation was limited to the rigid body translation along the yaw axis. Response in this direction would not be affected by excitation along the roll and pitch axes for this simple system, but would be affected by pitch (angular) acceleration. Examination of the input data indicates that the rotational excitation was of the same order of magnitude as the translational excitation. Figures 1–6 show the input and first mode responses in the time and frequency domains for cases 1 and 2.

Table 1 Modes and frequencies

Mode	Case 1 Frequency, Hz	Case 2 Frequency, Hz	Damping ratio	Mode shape Mass 1	Mode shape Mass 2	Mode shape Mass 3
1	15.0	20.3	0.025	0.1564	0.5316	1.0000
2	98.1	133.0	0.025	−0.8416	1.0000	0.6633
3	263.0	357.0	0.025	1.0000	−0.6990	0.2152

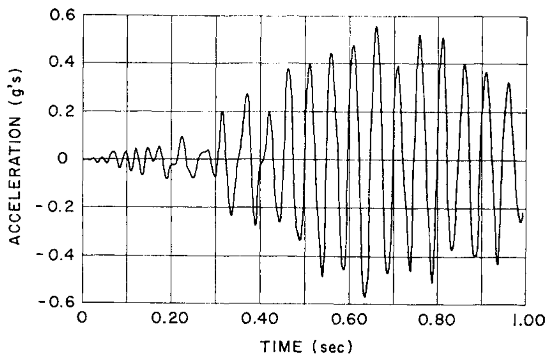

Fig. 1 Input acceleration (C-8).

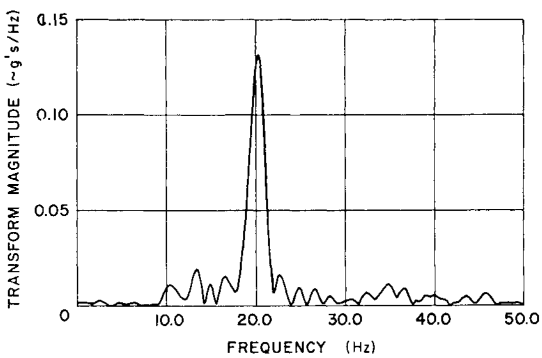

Fig. 2 Input acceleration spectrum.

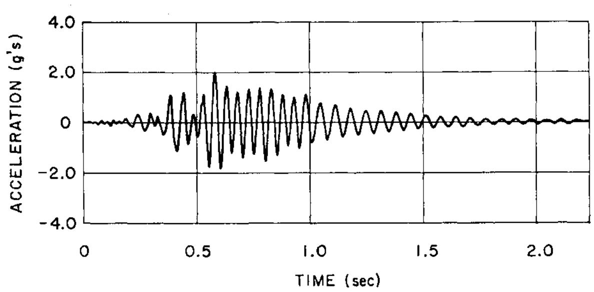

Fig. 3 Mode 1 acceleration (case 1).

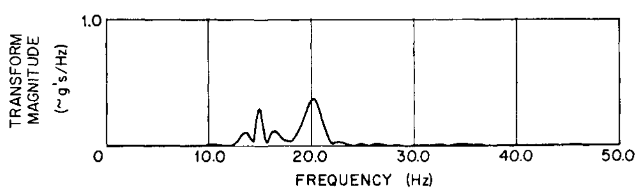

Fig. 4 Mode 1 acceleration spectrum (case 1).

Many of the 27 input spectra have spikes at or near 20.3 Hz, which is why this frequency was chosen for the case 2 first natural frequency. This characteristic is clearly seen in Fig. 2. Case 2 represents a most unfortunate design.

Case 1 represents fortunate design. The 15.0 Hz first natural frequency avoids spikes in the input spectra, although spikes fall nearby in some cases.

The second mode response was small compared to the first mode response (5% or less) and the third mode response was lower still. Therefore, the curves for mode 1 response accelerations can be taken to represent relative accelerations of the uppermost mass particle (mode 1 is normalized to unit displacement of this particle). In case 2, for which the

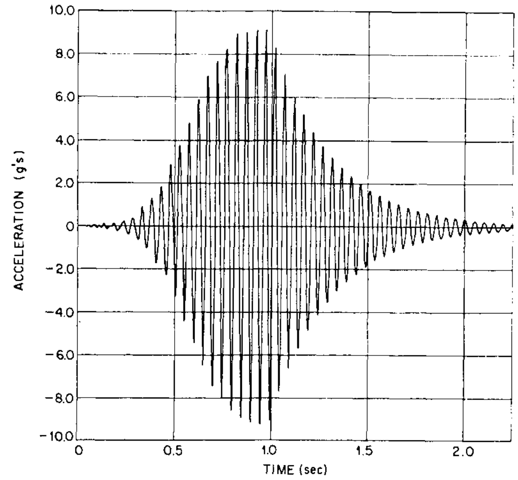

Fig. 5 Mode 1 acceleration (case 2).

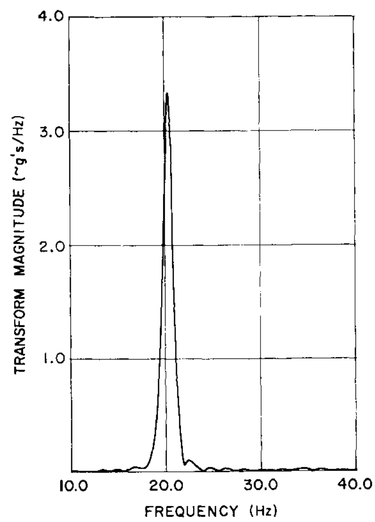

Fig. 6 Mode 1 acceleration spectrum (case 2).

excitation is resonant, the relative acceleration of the uppermost mass particle is indistinguishable from the absolute acceleration, but this is not true for case 1.

Bounding

From Eq. (9) it follows that

$$|f(t)| \leqq \int_{-\infty}^{\infty} |F(\omega)| \frac{d\omega}{2\pi} \tag{15}$$

Equation (15) states that the magnitude of the time function is bounded by the integral of the magnitude of its Fourier transform. The time functions here are real; therefore, their Fourier transforms have even real parts and odd imaginary parts and the magnitudes of their transforms are even functions of frequency. Hence, Eq. (15) can be written

$$|f(t)| \leqq 2\int_{0}^{\infty} |F(\omega)| \frac{d\omega}{2\pi} \tag{16}$$

Thus, the time function of Fig. 5, for example, is bounded by twice the area under the frequency function of Fig. 6.

To test the usefulness of this bound, the areas of the mode 1 response spectra were calculated for all 27 inputs for both case 1 and 2. The bound was found to exceed the actual maximum by 6–20% for cases in which resonance was quite clearly defined. In cases of low input without any predominant spectral peaks the bound exceeded the actual maximum by as much as 200%.

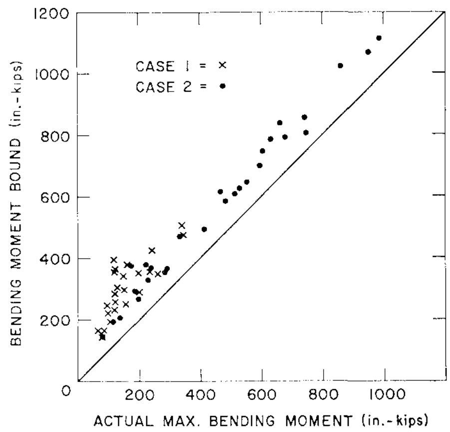

Fig. 7 Bending moment bounds.

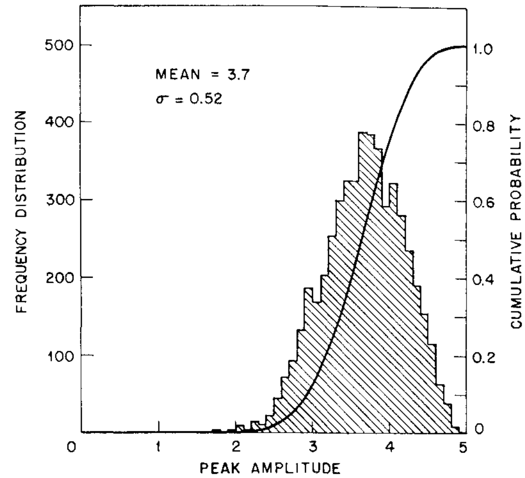

Fig. 8 Statistics of the peak amplitude of the sum of five enveloped cosine functions.

Figure 7 shows the nature of the bounding in another way. The abscissas are actual maximum bending moments and the ordinates are the corresponding bounds based on the assumption the bending moment is due to first mode acceleration only. The height of a given point above the 45° diagonal is the margin by which the bound exceeds the actual maximum. Thus, bounding could be quite useful in the early stages of design, especially if the possibility of resonance must be accepted.

Conclusions and Recommendations

It should now be apparent that valuable insight into system response can be gained from an excitation spectrum. The spectrum of a given time history is obtained easily and efficiently by the Fast Fourier transform.[4] Weighting the input for modal participation and multiplying by the appropriate transfer function yields the spectrum of the response. From this one can obtain a bound on the maximum response of the system or the complete time history of the response using the same Fast Fourier technique. Being able to obtain the actual time history of the response overcomes the real drawback of the familiar "shock spectrum" technique,[5] whereby the peak response of a multi-degree-of-freedom system must be estimated (often very conservatively) from the peak response as a function of frequency of a single-degree-of-freedom oscillator.

Completion of the study entails calculation of system response to all six components of rigid body input motion. For the simple system of this study, three response sets would be found, one for each of the coordinate directions. Presumably, only the first mode response would need to be considered for each direction. Calculation of the stress at the base of the beam would entail combining the three responses, which can be done in either the frequency or time domain.

A simple experiment in time phasing indicates that the tedious search in the time domain for the worst combination of the responses is unnecessary. Five cosine waves were constructed with random frequencies uniformly distributed between 5.0 and 30.0 Hz, and random phase angles uniformly distributed between 0 and 2π rad. Each cosine function was enveloped by $\frac{1}{2}(1 - \cos \pi t)$ to imitate an actual excitation (see next section). Summing the five cosines over one period of the envelope modeled the simultaneous application of five excitations with different frequencies and random phase. The peak amplitude of the summed cosines was noted. The experiment was repeated 5000 times to ensure that the mean value and standard deviation of the population of peak amplitudes was a good estimate for an infinite population (Fig. 8). Since the maximum possible sum of the five cosines was 5.0, the mean value represented 74% of the maximum.

The cumulative probability thus indicates that the occurrence of a peak which approaches the maximum individual sum must be allowed to warrant a high confidence level in system design. Thus, to ignore time phasing of the inputs and simply sum maximum individual responses would not appear to be too conservative.

Ignoring time phasing would be most advantageous for a complicated system where many member stresses might be desired. The maximum of each modal response should be found and then all member stresses or other desired results should be computed as linear combinations of these maxima.

In the early stages of satellite design, useful calculations can be made if the designer knows, roughly, the payload weight, outside dimensions and a band within which the lowest natural frequencies will lie. (If this information is unknown, it is hard to conceive of a mathematical theory that can help.) Assumptions can be made for mode shapes and frequencies for the first modes in bending (two directions), torsion and axial motion, and with a uniform distribution of mass throughout space occupied by the payload, the maximum acceleration of the center of gravity of the satellite can be found.

The Fourier transforms from several engine firings might be selected for input data. Engineering policy will influence which of the firings and what natural frequencies are selected. However, it is difficult to predict natural frequencies within 1 or 2 Hz, even when the design is known. Such errors can make a sizable difference in system response.

Mean Square Response to Nonstationary, Random Excitation

The techniques for calculation of low-frequency response of a structure to a well-defined, deterministic, transient dynamic excitation are well established. When the excitation is not deterministic, but is given as a nonstationary random process, calculation of the appropriate response statistics becomes a more formidable problem. Determination of the low-frequency response of a spacecraft when subjected to an excitation due to any one of the transient events that occur during the boost phase of a flight (e.g., booster engine cutoff) may be classified as a problem of the second kind.

A plan of analysis is laid out to determine the mean square response, as measured by deflections and member loads, of the spacecraft structure when subjected to a nonstationary, random, rigid body motion at its base. This excitation is modeled as a superpositioning of a finite number of enveloped, narrowband processes

$$\ddot{u}_0(t) = g_1{}^{\bar{u}}(t)n_1{}^{\bar{u}}(t) + g_2{}^{\bar{u}}(t)n_2{}^{\bar{u}}(t) + \cdots + g_{N\bar{u}}{}^{\bar{u}}(t)n_{N\bar{u}}{}^{\bar{u}}(t) \quad (18)$$

In these, $g(t)$ is some well defined, slowly varying, envelope function and $n(t)$ represents a narrowband, stationary process, assumed to exhibit an exponentially decaying harmonic correlation function as defined by Eq. (19):

$$E[n(t_1)n(t_2)] = R_n(t_2 - t_1) = R_0 e^{-\varepsilon\mu\Omega|t_2 - t_1|}\cos\Omega(t_2 - t_1) \quad (19)$$

The cross correlation of $n_i(t)$ and $n_j(t)$ is modeled in a similar way.

Assuming the above characterization of the excitation is appropriate, two problems remain: 1) given an ensemble of time histories of the excitation, $\ddot{u}_0(t), \ldots, \ddot{\theta}_z(t)$, establish a rational procedure for the calculation of an appropriate envelope function $g(t)$ and the parameters, e.g., R_0, μ, Ω, which describes the nature of the underlying, narrowband, stationary processes, and 2) calculate the mean square response.

It will be seen that with $g(t)$ "slowly varying," that is, changes in $g(t)$ of order 1.0 occur over a time period $1./\varepsilon\Omega$ of order 1.0, considerable simplification is attained in the solution of these two problems.

General Formulation of Mean Square Response Problem

Rewriting Eq. (3) in matrix form yields

$$\{\ddot{\xi}\} + [\ 2\zeta\omega_k\ ]\{\dot{\xi}\} + [\ \omega_k{}^2\ ]\{\xi(t)\} = -[\Gamma]\{F(t)\} \quad (20)$$

where $F(t)$ is now a column matrix of the six rigid body interface accelerations defined by Eq. (18). For any one model participation function, the response may be written via Duhamel's integral as

$$\xi(t) = \int_0^t h(t, t_1)[\Gamma_{\bar{u}}\ddot{u}_0(t_1) + \Gamma_{\bar{v}}\ddot{v}_0(t_1) + \cdots + \Gamma_{\theta_z}\ddot{\theta}_z(t_1)]dt_1 \quad (21)$$

where $h(t, t_1)$ is the impulse response of the system. Using Eq. (18) and assuming the envelope functions to be the same for convenience, the mean square response has the form

$$\begin{aligned} E[\xi^2(t)] = {} & \Gamma_{\bar{u}}{}^2 \int_0^t\int_0^t h(t, t_1)h(t, t_2)g(t_1)g(t_2) \cdot \{E[n_1{}^{\bar{u}}(t_1)n_1{}^{\bar{u}}(t_2)] + \\ & E[n_1{}^{\bar{u}}(t_1)n_2{}^{\bar{u}}(t_2)] + E[n_1{}^{\bar{u}}(t_2)n_2{}^{\bar{u}}(t_1)] + \cdots + \cdots \\ & E[n_{N\bar{u}}{}^{\bar{u}}(t_1)n_{N\bar{u}}{}^{\bar{u}}(t_2)]\}dt_1dt_2 + \\ & \Gamma_{\bar{u}}\Gamma_{\bar{v}}\int_0^t\int_0^t h(t, t_1)h(t, t_2)g(t_1)g(t_2) \cdot \\ & \{E[n_1{}^{\bar{u}}(t_1)n_1{}^{\bar{v}}(t_2)] + E[n_1{}^{\bar{u}}(t_2)n_1{}^{\bar{v}}(t_1)] + \cdots\}dt_1dt_2 + \cdots \end{aligned} \quad (22)$$

Assuming the parameters associated with the auto- and cross-correlations of the underlying stationary narrowband processes have been determined, one may compute the mean square modal participation response from the foregoing. However, the difficulty of performing the indicated operations should be apparent.

Since the member loads are related by a linear transformation to modal displacements and rotations which, in turn, are related to the modal participation functions via another linear transformation involving the matrix of normal modes, the mean square response of any one member load is given by

$$E[\sigma^2(t)] = \sum_{i=1}^{N}\sum_{j=1}^{N} b_{ij}E[\xi_i(t)\xi_j(t)] \quad (23)$$

where N is the number of normal modes retained and b_{ij} is symmetric. One must thus compute the correlation of the modal participation functions as well as the mean square response of any one mode. The required relationships for this computation are similar to Eq. (22).

The general plan of analysis is a formidable task. To illustrate the simplification afforded to this task by the process of idealization of the excitation as a superpositioning of a number of enveloped, stationary narrowband processes, the next section gives as an example the response of a single-degree-of-freedom system to a single enveloped, narrowband excitation.

Single-Degree-of-Freedom Response

Formulation

Again, begin with a second-order system as described by

$$\ddot{\xi}(t) + 2\zeta\omega_k\dot{\xi}(t) + \omega_k{}^2\xi(t) = \omega_k{}^2 f(t)$$

where $f(t)$ is taken in the form

$$f(t) = g(t) \cdot n(t) \quad (24)$$

Assuming the system is initially at rest, the mean square response, as a function of time, obtained from an ensemble averaging procedure is

$$\begin{aligned} E[\xi^2(t)] = \omega_k{}^2\left(\frac{\omega_k}{\omega_d}\right)^2 \int_0^t\int_0^t e^{-\zeta\omega_k(t-t_1)} \cdot \\ \sin\omega_d(t - t_1)e^{-\zeta\omega_k(t-t_2)}\sin\omega_d(t - t_2) \cdot \\ g(t_1)g(t_2)R_n(t_2 - t_1)dt_1dt_2 \end{aligned} \quad (25)$$

In this, ω_d is the damped natural frequency of the system

$$\omega_d = \omega_k(1 - \zeta^2)^{1/2}$$

In the future ω_d will be set equal to the natural frequency ω_k since ζ is assumed small.

$$\zeta = \varepsilon \ll 1.0 \quad (26)$$

With $R_n(t_2 - t_1)$ taken in the form

$$R_n(t_2 - t_1) = R_0 e^{-\varepsilon\mu\Omega|t_2 - t_1|}\cos\Omega(t_2 - t_1) \quad (27)$$

where μ is of the order one, i.e., a narrowband process, the mean square response becomes

$$\begin{aligned} E[\xi^2(t)] = R_0\omega_k{}^2 e^{-2\varepsilon\omega_k t}\int_0^t\int_0^t g(t_1)g(t_2) \\ e^{-\varepsilon\mu\Omega|t_2-t_1|}\cos\Omega(t_2 - t_1)\cdot e^{+\varepsilon\omega_k(t_1+t_2)}\sin\omega_k(t - t_1) \cdot \\ \sin\omega_k(t - t_2)dt_1dt_2 \end{aligned} \quad (28)$$

If this envelope function may be characterized as "slowly varying" in the sense previously defined, considerable simplification is attained as follows:

$$\tau_i = \varepsilon\omega_k t_i, \qquad i = 1, 2, \qquad \eta = \varepsilon\omega_k t \quad (29)$$

Equation (28) becomes

$$\begin{aligned} E[\xi^2(\eta)] = \frac{R_0 e^{-2\eta}}{\varepsilon^2}\int_0^\eta\int_0^\eta e^{(\tau_1+\tau_2)}\sin\left(\frac{\eta - \tau_1}{\varepsilon}\right) \\ \cdot \sin\left(\frac{\eta - \tau_2}{\varepsilon}\right)g(\tau_1)g(\tau_2)e^{-\mu\lambda|\tau_2-\tau_1|} \\ \cdot \cos\frac{\lambda(\tau_2 - \tau_1)}{\varepsilon}d\tau_1d\tau_2 \end{aligned} \quad (30)$$

where $\lambda = \Omega/\omega_k$.

Two cases are now considered: (1) $\lambda \cong 1.0$, (2) $\lambda \neq 1.0$. In the first case, setting

$$\lambda = 1 + \varepsilon\beta \quad (31)$$

yields[6]

$$E[\xi^2(\eta)] = \frac{R_0}{4\varepsilon^2}\{e^{-2\eta}\int_0^\eta\int_0^\eta e^{(\tau_1+\tau_2)}\cdot$$
$$e^{-\mu\lambda|\tau_2-\tau_1|}g(\tau_1)g(\tau_2)\cos\beta(\tau_2-\tau_1)\cdot d\tau_1 d\tau_2 + O(\varepsilon)\} \quad (32)$$

When λ is not in the vicinity of 1.0 one obtains[6]

$$E[\xi^2(\eta)] = \frac{R_0}{(\lambda^2-1)^2}\{g^2(\eta) + \mu\lambda(1+\lambda^2)$$
$$\cdot e^{-2\eta}\int_0^\eta e^{2\tau}g^2(\tau)d\tau + O(\varepsilon)\} \quad (33)$$

[In obtaining this, $g(0)$ is assumed to be zero.] Note that the relative orders of magnitude of the mean square response in these two cases is as expected.

Determination of R_0, μ, and Ω

The energy density spectrum of any one member of the ensemble of forcing functions may be written

$$F(\omega)\cdot F^*(\omega) = \int_{-\infty}^{+\infty}\int_{-\infty}^{+\infty} e^{-i\omega(t_1-t_2)}\cdot f(t_1)f(t_2)dt_1dt_2 \quad (34)$$

Taking the ensemble average (the expected value of this quantity) gives

$$E[F(\omega)\cdot F^*(\omega)] = \int_{-\infty}^{+\infty}\int_{-\infty}^{+\infty} e^{-i\omega(t_1-t_2)}\cdot$$
$$g(t_1)g(t_2)R_0e^{-\varepsilon\mu\Omega|t_2-t_1|}\cdot\cos\Omega(t_2-t_1)dt_1dt_2 \quad (35)$$

The left-hand side of this expression is computed from the actual ensemble of forcing function time histories. The right-hand side becomes, upon selection of $g(t)$ and integrating, a function of the parameters R_0, μ, and Ω. In this procedure, the fact that $g(t)$ is slowly varying again affords some simplification of the required integration.

In the examples considered, Ω was chosen as that value of frequency where the mean of the energy density spectrum attained a maximum. Having chosen an appropriate envelope function, evaluating Eq. (35) at the peak and half-power points yielded two additional, in general, coupled, transcendental equations for R_0 and μ. Having these parameters, Eq. (32) or (33), depending upon λ, yielded the desired mean square response.

Example B

The excitation chosen for this example was taken as the ensemble of the 27 yaw axis, booster/payload interface accelerations, $f(t) = \ddot{w}_0(t)$. The envelope function $g(t)$ was chosen as:

$$g(t) = \tfrac{1}{2}(1-\cos\omega_0 t) \quad (36)$$

where $\omega_0 = 0.704$ Hz. Superimposed in Fig. 9 are several

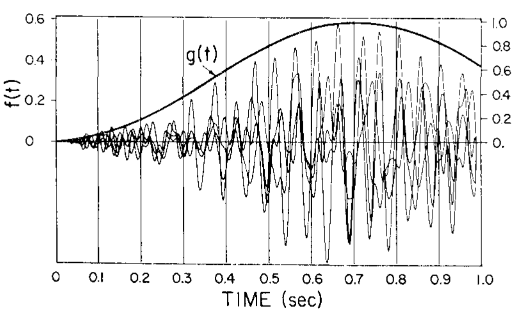

Fig. 9 Several representative excitation time histories $f(t)$ and envelope function $g(t)$.

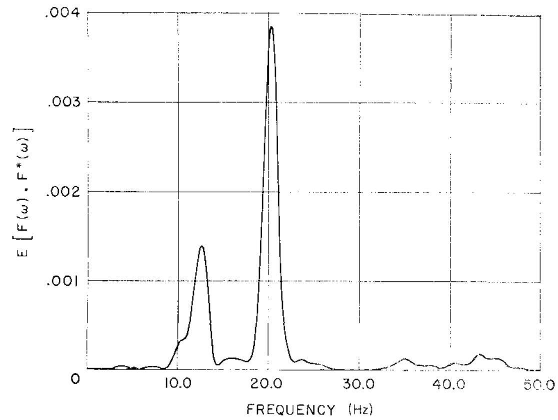

Fig. 10 Mean energy density spectrum of the excitation.

representative time histories of $\ddot{w}_0(t)$ together with a plot of $g(t)$.

The expected value of the energy density spectrum of the ensemble (Fig. 10) shows $\Omega = 20.33$ Hz. Evaluation of Eq. (35) at the peak and half-power points yielded

$$R_0 = 0.0381;\ \mu = 0.9457 \quad (37)$$

The response was determined for the following three cases: 1) $\beta = 0.0$; $\omega_k = 20.33$ cps, $\zeta = .025$; 2) $\beta = 2.0$; $\omega_k = 21.35$ cps, $\zeta = .025$; and 3) $\beta = 4.0$; $\omega_k = 22.37$ cps, $\zeta = .025$. In the first case, the system was tuned to the center frequency of the taller of the two peaks observed in the plot of the mean energy density spectrum. In the remaining two cases, the system was tuned to the same area. With this choice of parameters the effect of the enveloped, narrowband process centered at the lower peak frequency, ~13 Hz, should be negligible according to Eqs. (32) and (33). Furthermore, it can be shown that the contribution of the cross correlation to the response of these two enveloped, narrowband signals is also negligible.

The results of this analysis are displayed in Figs. 11–13 where the 27 response time histories, as computed from a numerical solution of the differential equation, have been superimposed. Shown also is the root mean square response (σ) obtained from the solution of Eq. (32) and the 3σ response as functions of time. Observe that the 3σ time histories closely envelope the superimposed response time histories.

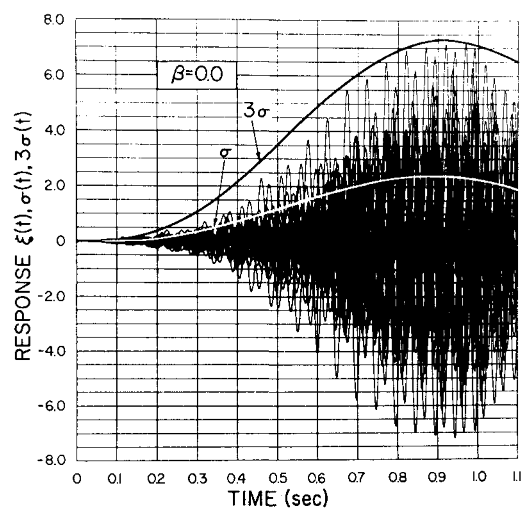

Fig. 11 Response time histories $\xi_j(t), j = 1, 27$ and rms response time history, $\sigma(t)$, for $\beta = 0.0$.

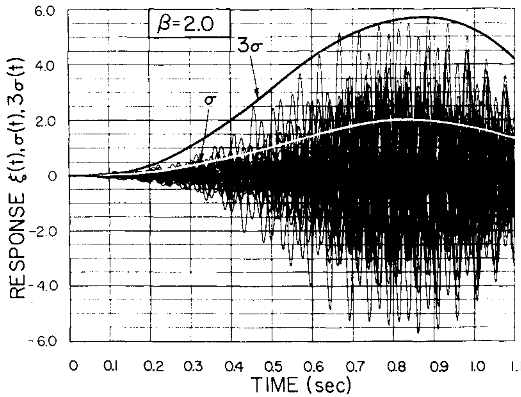

Fig. 12 Response time histories $\xi_j(t), j = 1, 27$ and rms response time history, $\sigma(t)$, for $\beta = 2.0$.

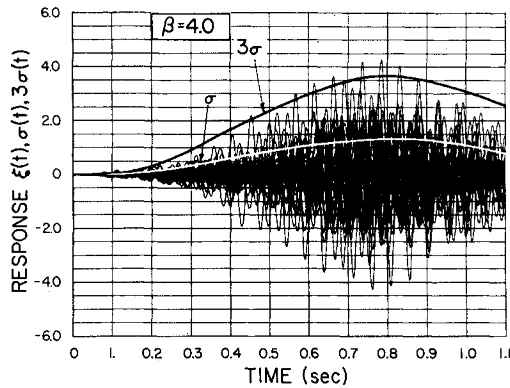

Fig. 13 Response time histories $\xi_j(t), j = 1, 27$ and rms response time history, $\sigma(t)$, for $\beta = 4.0$.

Conclusions and Recommendations

The preceding simple example indicates that the approach proposed for the determination of the response of a structure to nonstationary excitation has merit, and suggests a rational way to establish an equivalent nonstationary, random excitation, given an ensemble of interface acceleration time histories. Modeling this environment as a superpositioning of a finite number of enveloped, stationary narrowband processes, where the envelope is slowly varying, is seen to lead to considerable simplification in calculating the mean square response. Although, in the example treated, a single enveloped process was assumed, the conditions for this simplification remain in the general problem. Note also, that according to Eqs. (32) and (33), integration was carried out with respect to the slow time variable, $\eta = \varepsilon\omega t$. If a numerical scheme is established for the general problem, this last aspect of this approach implies that the time increment size can be quite large compared to the period of the underlying narrowband process in the excitations.

References

[1] Turney, R. L., private communication, Aug. 1967, Martin Marietta Corp., Denver, Colo.

[2] Uchiyama, J. T., private communication, Dec. 1968, Martin Marietta Corp., Denver, Colo.

[3] Bracewell, R., *The Fourier Transform and Its Applications*, McGraw-Hill, New York, 1965.

[4] Cochran, W. T., "What is the Fast Fourier Transform?," *IEEE Transactions on Audio and Electroacoustics*, Vol. AU-15, No. 2, June 1967, pp. 45–55.

[5] Digeness, I., "Elementary Considerations of Shock Spectra," *Shock and Vibration Bulletin*, Vol. 34, Pt. 3, Dec. 1964, pp. 211–222.

[6] Bucciarelli, L. L., Jr. and Kuo, C., "Mean Square Response of a Second Order System to Nonstationary Random Excitation," *Transactions of the ASME, Ser. E: Journal of Applied Mechanics*, Vol. 37, No. 3, Sept. 1970, pp. 612–616.

[7] Mason, S. J. and Zimmerman, H. J., *Electronic Circuits, Signals, and Systems*, Wiley, New York, 1966.

[8] Bendat, J. S. and Piersol, A. G., *Measurement and Analysis of Random Data*, Wiley, New York 1966.